

Advanced Magnetometer System

MR-2646

Dr. Rahul Mhaskar and Dr. Rui Zhang

Geometrics, Inc.

In-Progress Review Meeting

May 16, 2018



MR-2646: Advanced Magnetometer System

**Performers: Dr. Rahul Mhaskar and Dr. Rui Zhang
Geometrics, Inc.**

Technology Focus

- Operate scalar atomic magnetometer in tandem with electromagnetic pulse transmitter coils for in-field UXO discrimination.

Research Objectives

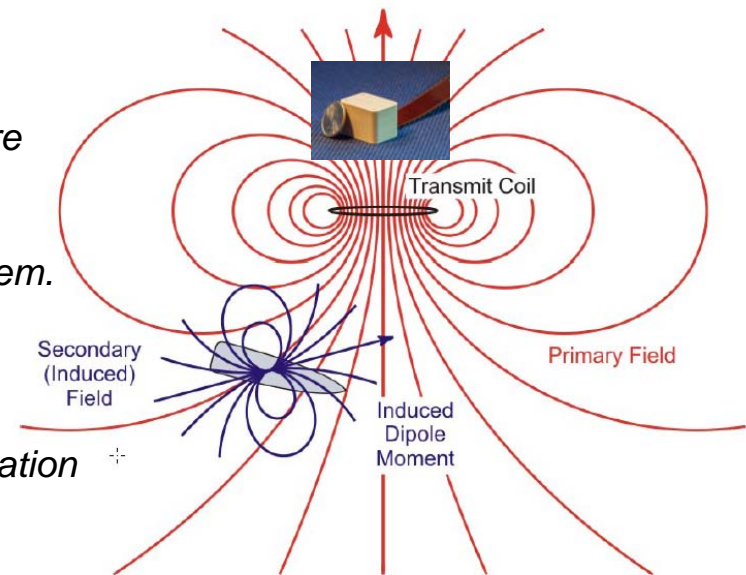
- Evaluate advanced methods of signal extraction in the miniature scalar magnetometer to obtain magnetic field orientation and electromagnetic pulse onset information leading to rapid DC magnetometer measurements in the presence of a TDEM system.

Project Progress and Results

- Measured vector field information from a scalar magnetometer
- Demonstrated sub-millisecond recovery of magnetometer operation after an electromagnetic pulse
- Simulated UXO response to multi-directional DC excitation

Technology Transition

- Geometrics is committed to integrating this new development with the MFAM miniature magnetometer technology, which is already commercialized and used by the industry and government users.



Social Media Content

- **Precision scalar miniature magnetometers under development by Geometrics will soon give you vector field information**
 - *Geometrics is developing technology to extract vector field information using the MFAM miniature magnetometer platform.*
 - *Offsets any need to provision for vector sensors like GMR or fluxgate magnetometers in system design to obtain orientation information.*
- **Laboratory experiments at Geometrics, Inc. demonstrate scalar magnetometers with ultra-fast operational recovery from disturbances caused by electromagnetic pulses.**
 - *The MFAM miniature magnetometers will now be able to make measurements within a millisecond of an electromagnetic pulse transmitted by an energized coil.*
 - *The MFAM miniature magnetometers in the near future can be used to measure the response from a Time-Domain Electromagnetic (TDEM) system, potentially obviating the need for large pick-up coils in near-surface resistivity surveys.*

Project Team

- Dr. Rahul Mhaskar
 - ◆ Sr. Scientist, Geometrics, Inc.
 - ◆ Technical lead
- Dr. Rui Zhang
 - ◆ Physicist, Geometrics, Inc.
 - ◆ Specialist in atomic magnetometry and optical physics
- Mr. Ken Smith
 - ◆ Sr. Electronics Engineer, Geometrics, Inc.
 - ◆ Expert in magnetometer system design and DSP
- Dr. Mark Prouty
 - ◆ President, Geometrics, Inc.
 - ◆ Technical and technology transfer supervision

Problem Statement

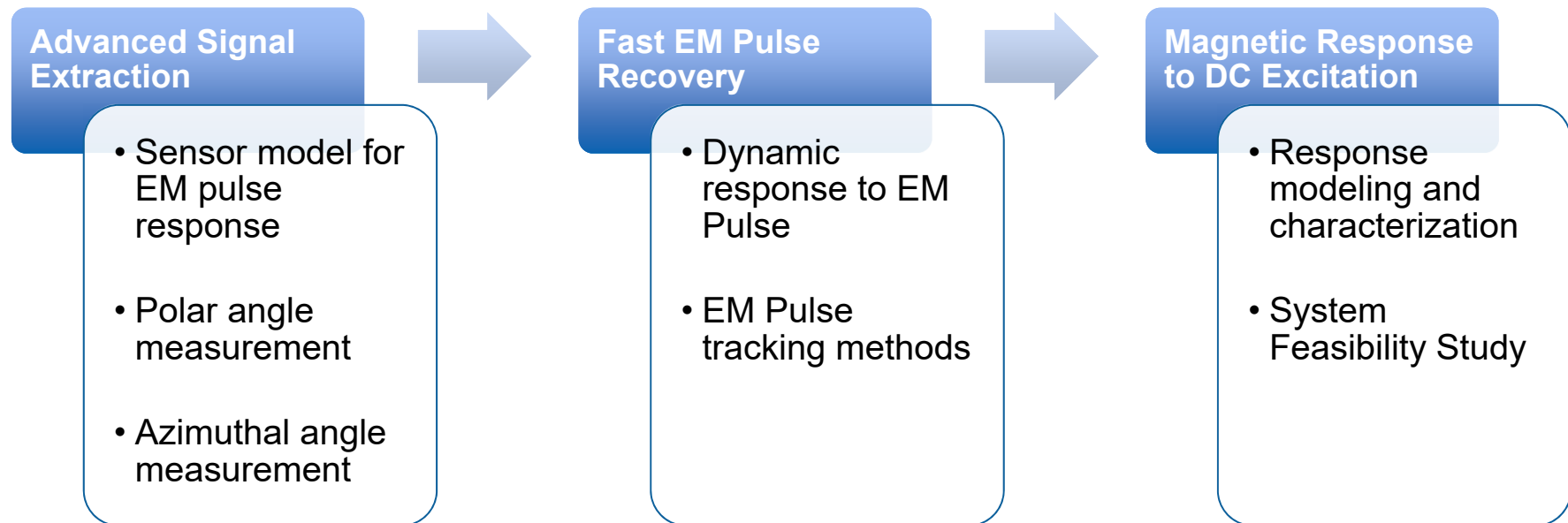
- **This technology is intended to improve remediation of military munitions underwater**
- **Time-Domain Electromagnetic (TDEM) systems proven to be effective technologies for overland UXO detection and classification**
- **Scalar atomic magnetometers are sensors of choice, particularly in marine environment**
- **Currently not possible to run both sensors simultaneously**
- **How to extend atomic magnetometer technology to function in presence of EM transmitter?**
- **How to utilize information made available by enabling such technology to advance underwater UXO remediation efforts?**

Technical Objective

Develop advanced methods of operating scalar atomic magnetometer in tandem with electromagnetic pulse transmitter coils

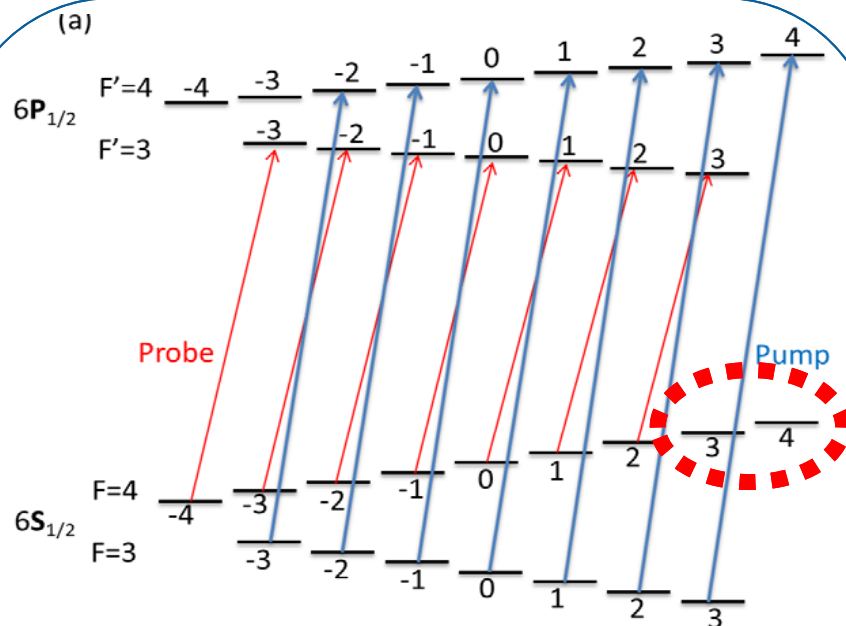
Investigate discrimination of UXO utilizing this capability for multi-directional DC magnetic measurements

Technical Approach

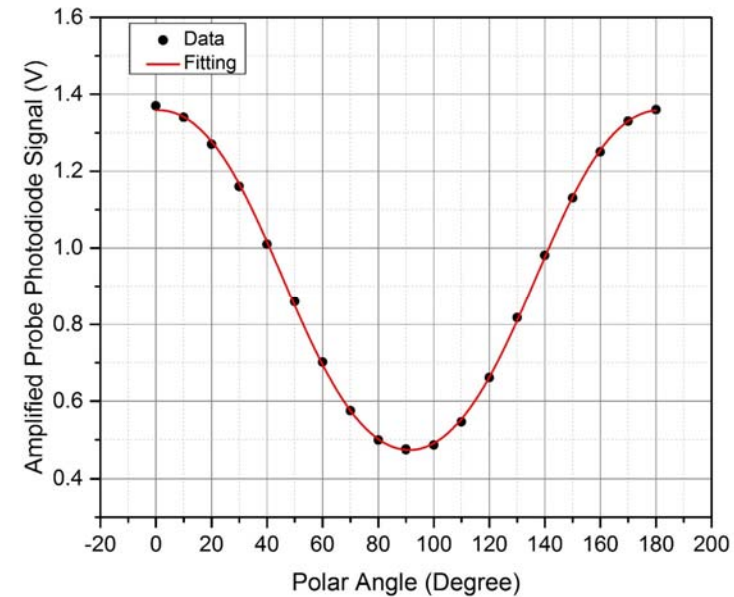


Advanced Signal Extraction

- Sensor Model and response of light absorption to polar angle



$|F=4, m=3\rangle$ and $|F=4, m=4\rangle$ are dark states for the probe. When the beam and the magnetic field are aligned, atoms will accumulate in the dark states, greatly reducing the absorption of the probe light.



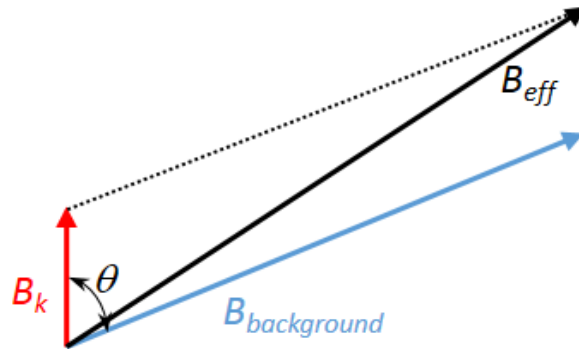
Nonlinear fit of the following equation:

$$y = A * \exp[-B * \sin^2 \theta - C * \sin^4 \theta] \quad (1)$$

yields good agreement with the data. Therefore, the polar angle can be calculated from the transmitted probe DC signal, according to the Equation (1).

Advanced Signal Extraction

- Response of light-shift-induced magnetic field to polar angle



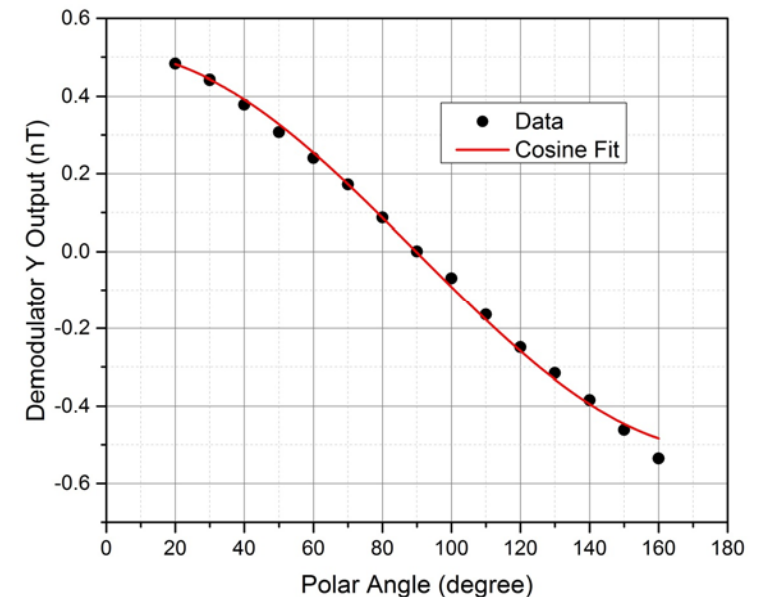
Light-shift due to the probe light acts as an effective magnetic field, B_k , along the probe direction. The total effective B measured by the magnetometer is:

$$B_{eff} = \sqrt{B^2 + B_k^2 + 2\cos\theta B B_k} \approx B + \cos\theta B_k \quad (2)$$

Complementary to the Absorption Method

1. Remove the ambiguity between θ and $180^\circ - \theta$
2. Improve the sensitivity around 90° polar angle

Projected Light-shift vs Polar Angle

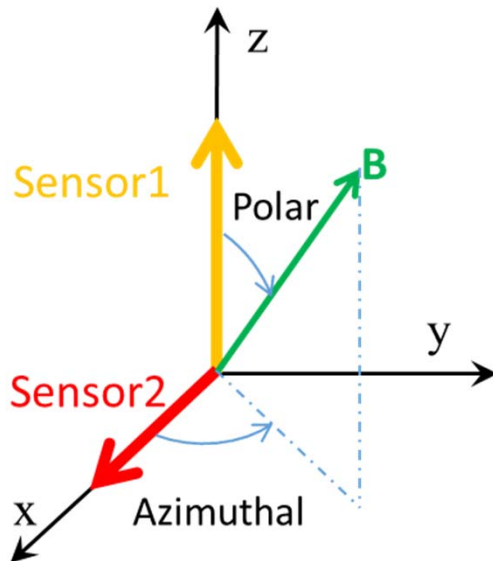


The experimental data is fitted well with a cosine function.

Advanced Signal Extraction

- Azimuthal angle measurement

Azimuthal Angle Measurement with Two Sensors



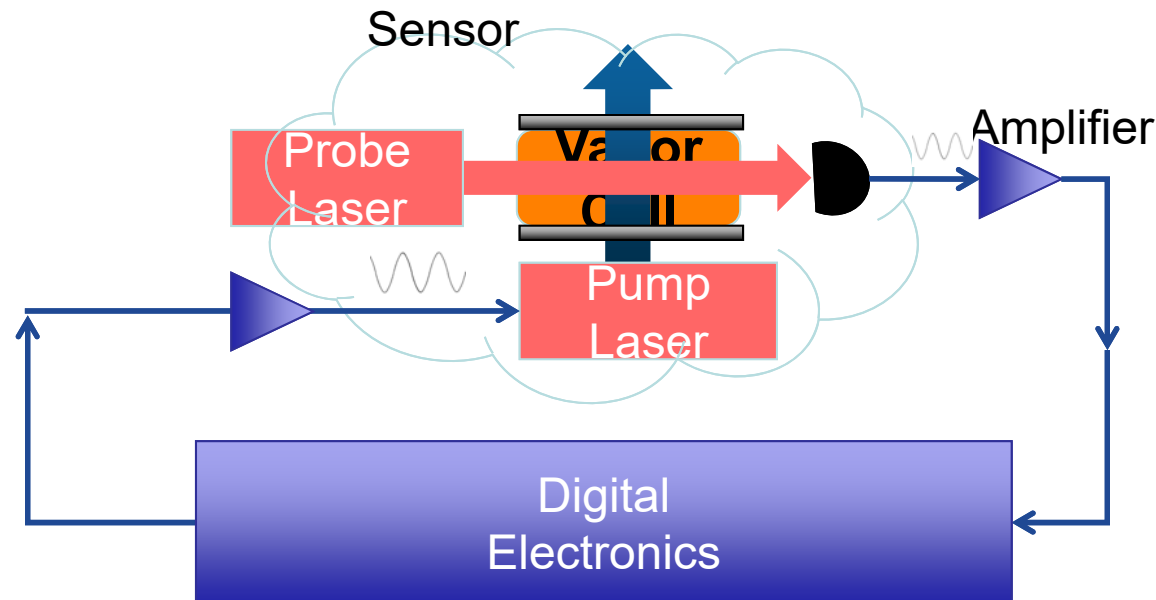
It can be calculated that the azimuthal angle of the magnetic field follows:

$$\cos \varphi = \frac{\cos \theta_2}{\sin \theta_1} \quad (3)$$

Here θ_1 and θ_2 are the polar angles of sensor 1 and sensor 2, respectively.

Fast EM Pulse Recovery

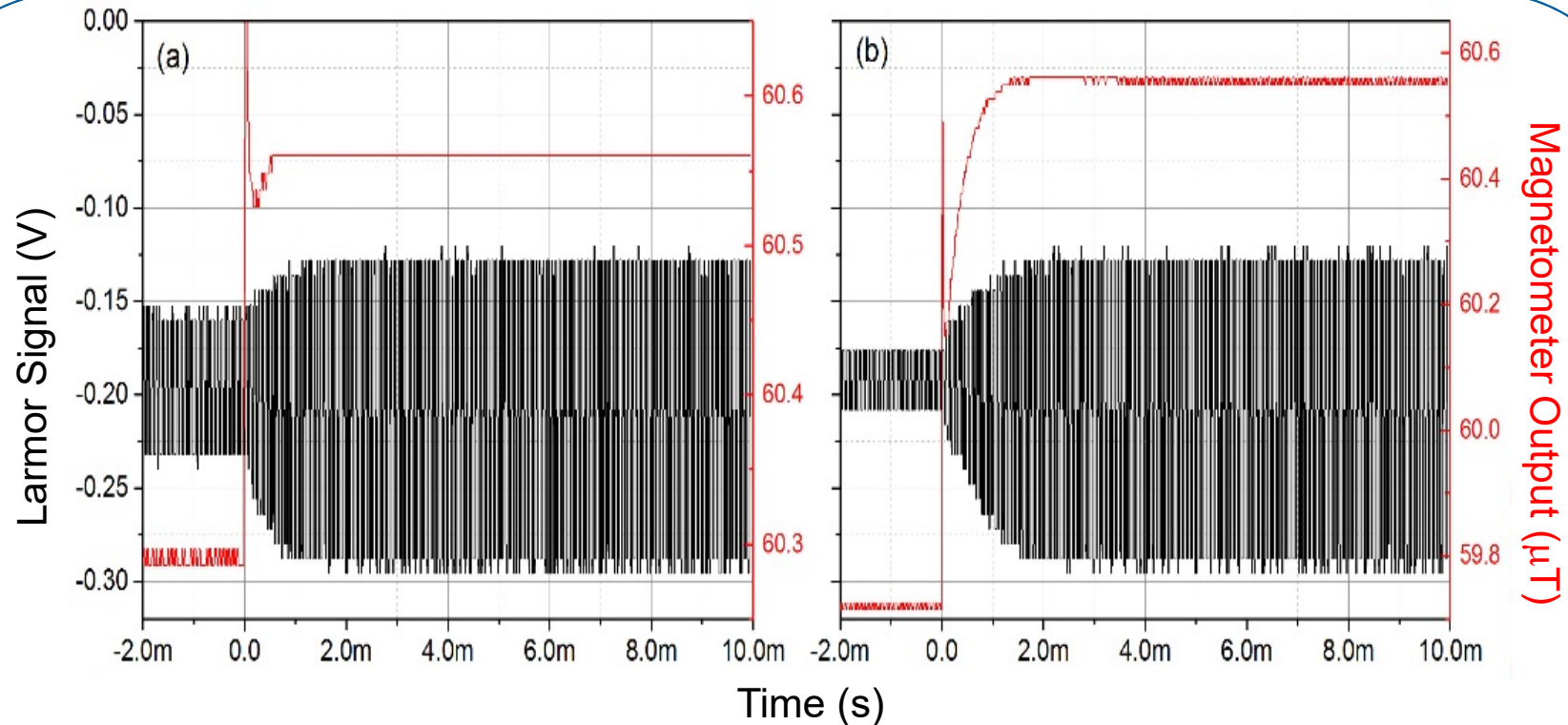
- Digital Signal Processing



Digital phase lock loop (PLL) to track the Larmor frequency of atoms in the vapor cell. The loop can be briefly suspended at the onset of the EM pulse and resumed at the end of the pulse. Fast-recovery is possible when the initial pump modulation frequency is close to the Larmor frequency when the PLL is re-engaged.

Fast EM Pulse Recovery

- Recovery time dependence on the initial pump modulation frequency

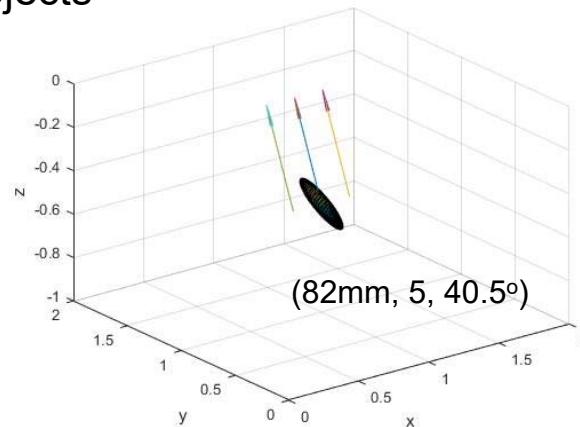
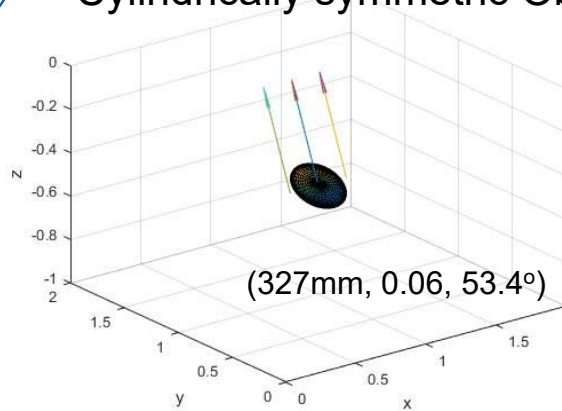


PLL is engaged at time = 0. Black curve is the detected Larmor signal and the red curve is the magnetometer output. (a) Initial pump modulation frequency 1 kHz away from the Larmor frequency. (b) 3 kHz difference.

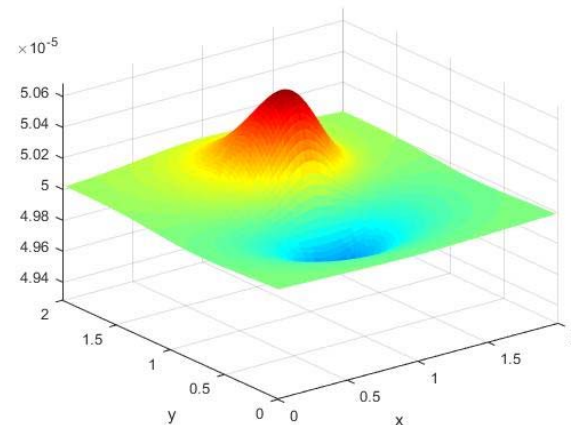
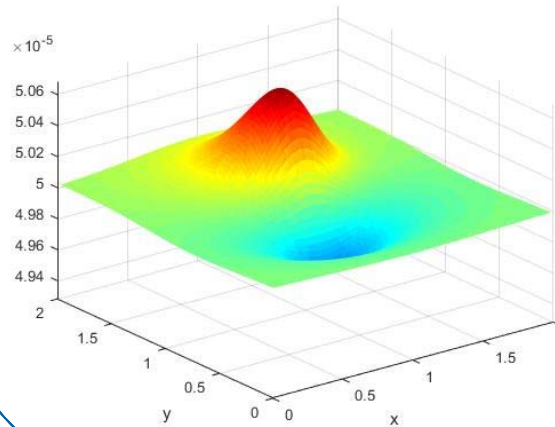
Magnetic Response to DC Excitation

- UXO discrimination enhancement with an additional quasi-DC magnetic field

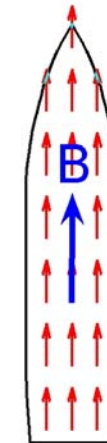
Cylindrically symmetric Objects



Corresponding Magnetic Response



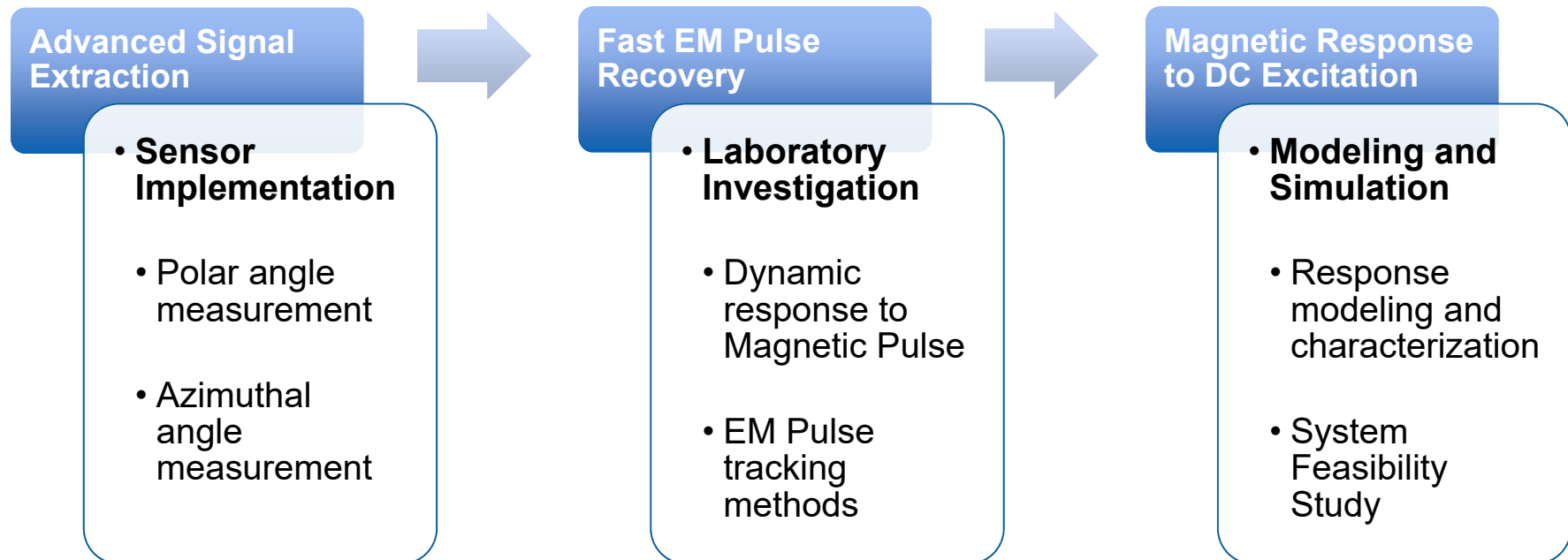
Some different shaped objects can have very



generated to change the total field direction.

Animation courtesy Dr. Stephen Billings

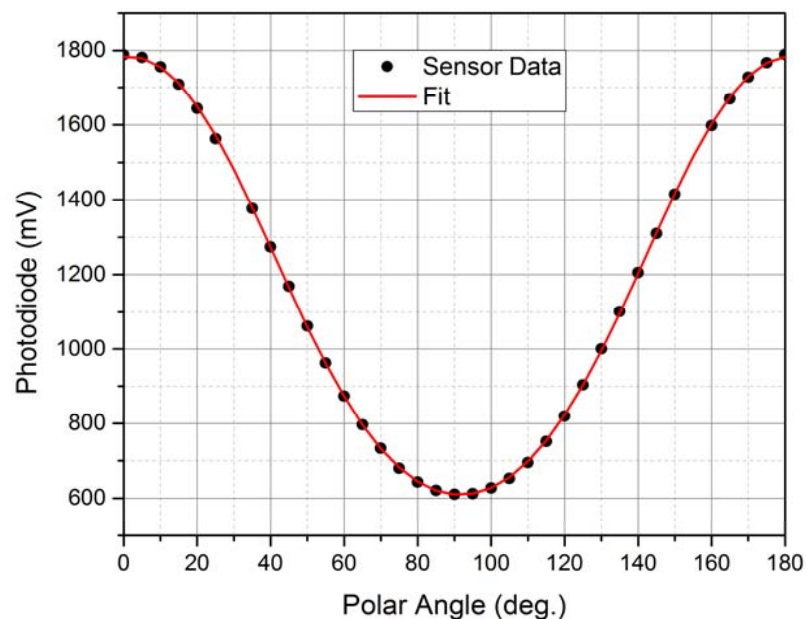
Results



Advanced Signal Extraction

- Light Absorption Method to measure Polar Angle

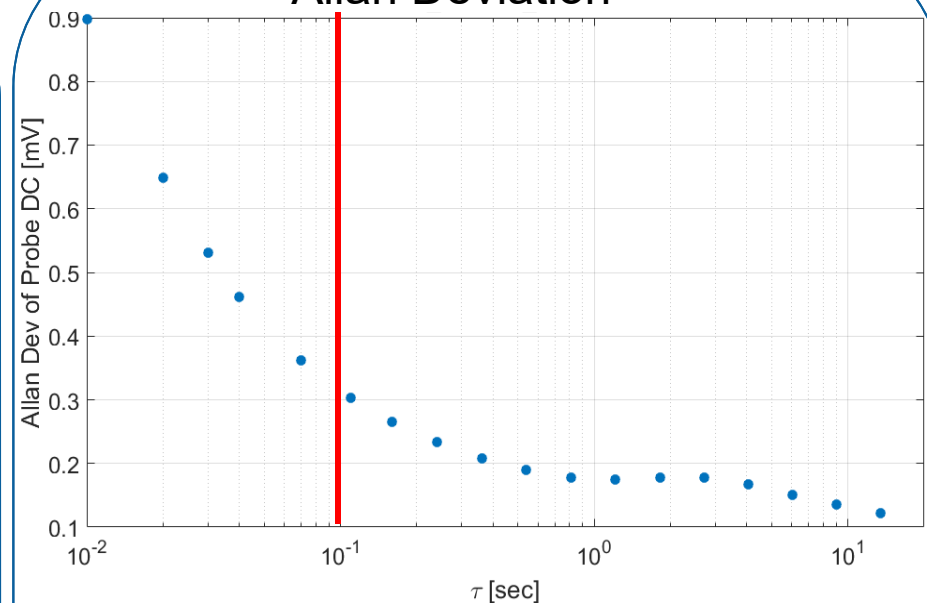
Probe DC in a MFAM sensor as a function of polar angle



Red curve is the fit of

$$y = A * \exp[-B * \sin^2 \theta - C * \sin^4 \theta] \quad (1)$$
to the sensor data.

Allan Deviation



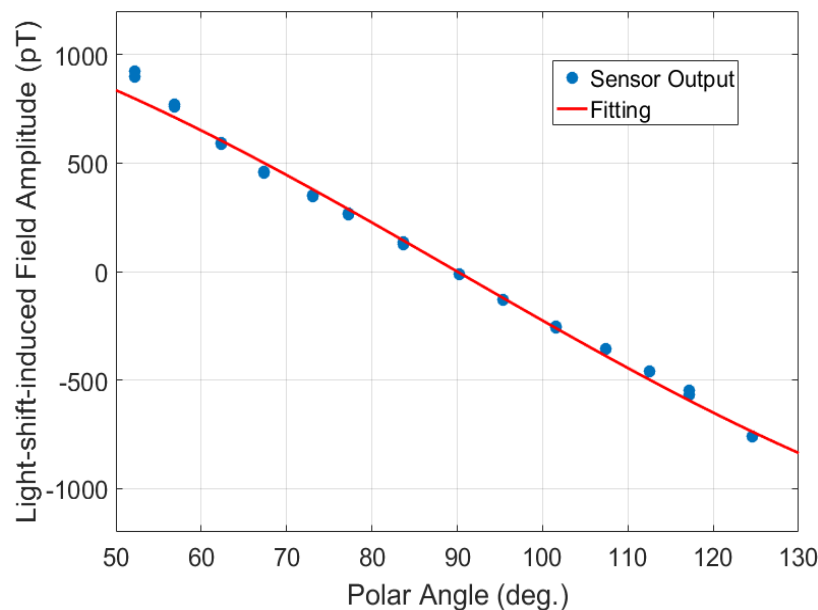
Resolution of the polar angle measurement can be better than **0.02°**.

- With an integration time of over 100 ms, the deviation of the probe DC drops below 0.3 mV.
- The slope of the left curve is about 0.05 degree/mV around 45° polar angle.

Advanced Signal Extraction

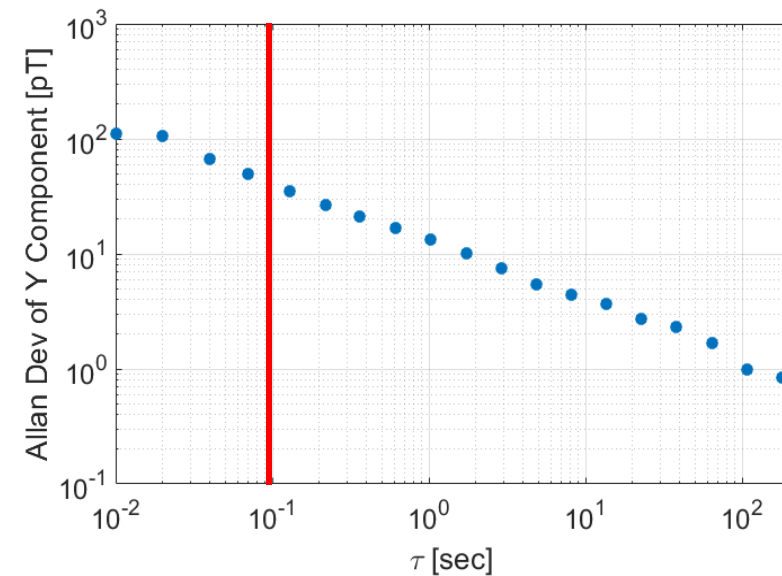
- Light-shift Method to measure Polar angle

Amplitude of Light-shift-induced Oscillating Field vs Polar Angle



A cosine function fit yields good agreement for angles around 90°.

Allan Deviation of the Amplitude



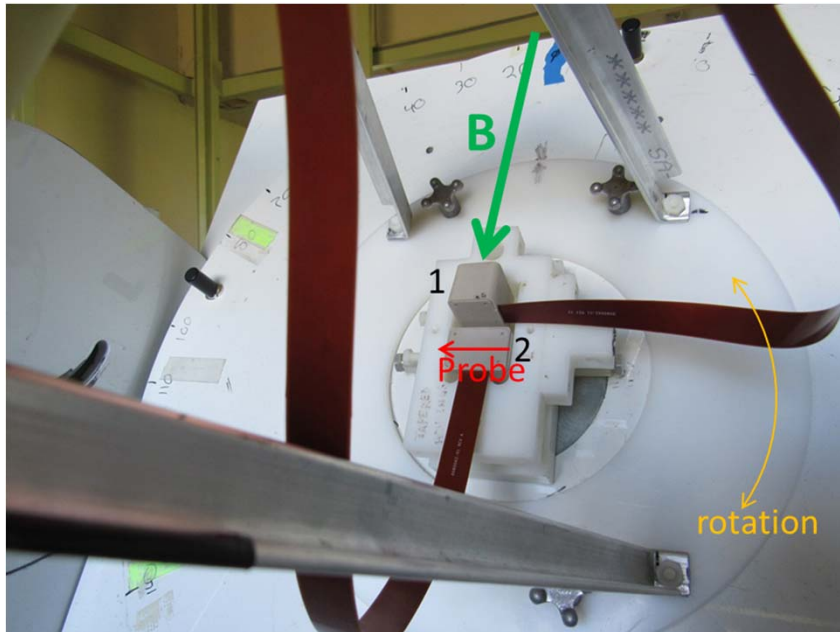
Resolution of the polar angle measurement is 2°.

- With a 100ms integration time, the deviation of the amplitude is about 40 pT.
- The slope of the left curve is about 0.05 degree/pT around 90° polar angle.

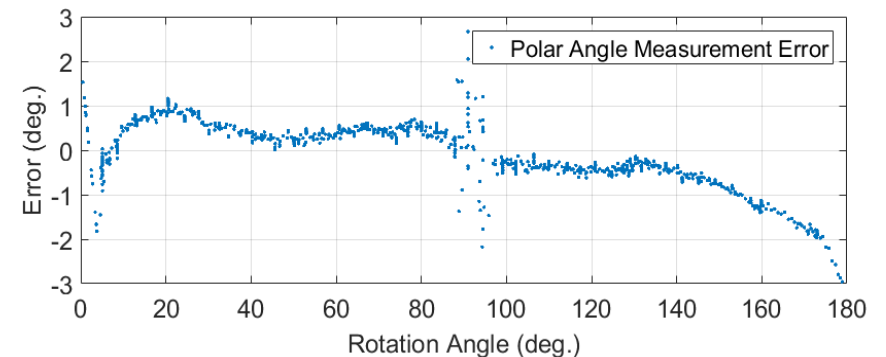
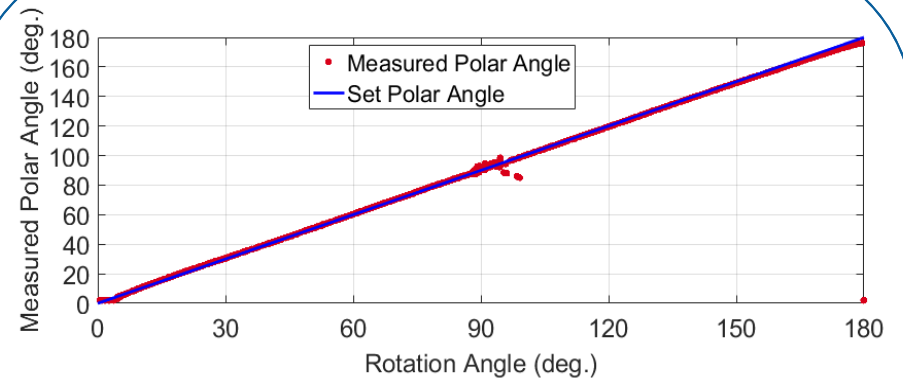
Advanced Signal Extraction

- Polar Angle Measurement using composite methods

Testing Structure at NASA



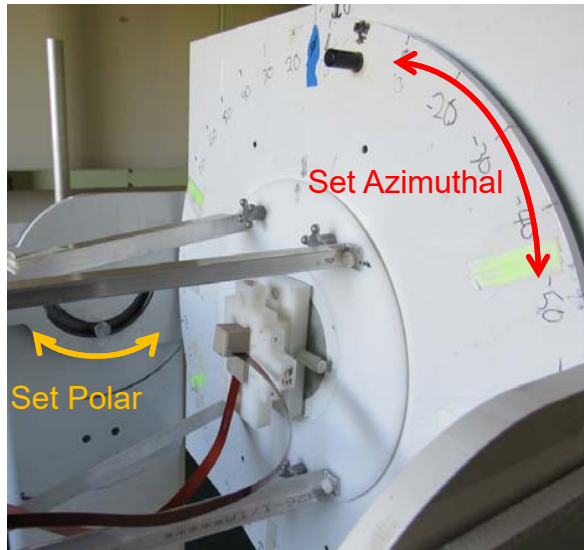
Rotation angle is recorded with an optical encoder with a resolution of 0.35° . Measured polar angle of sensor 2 is compared with the rotation angle.



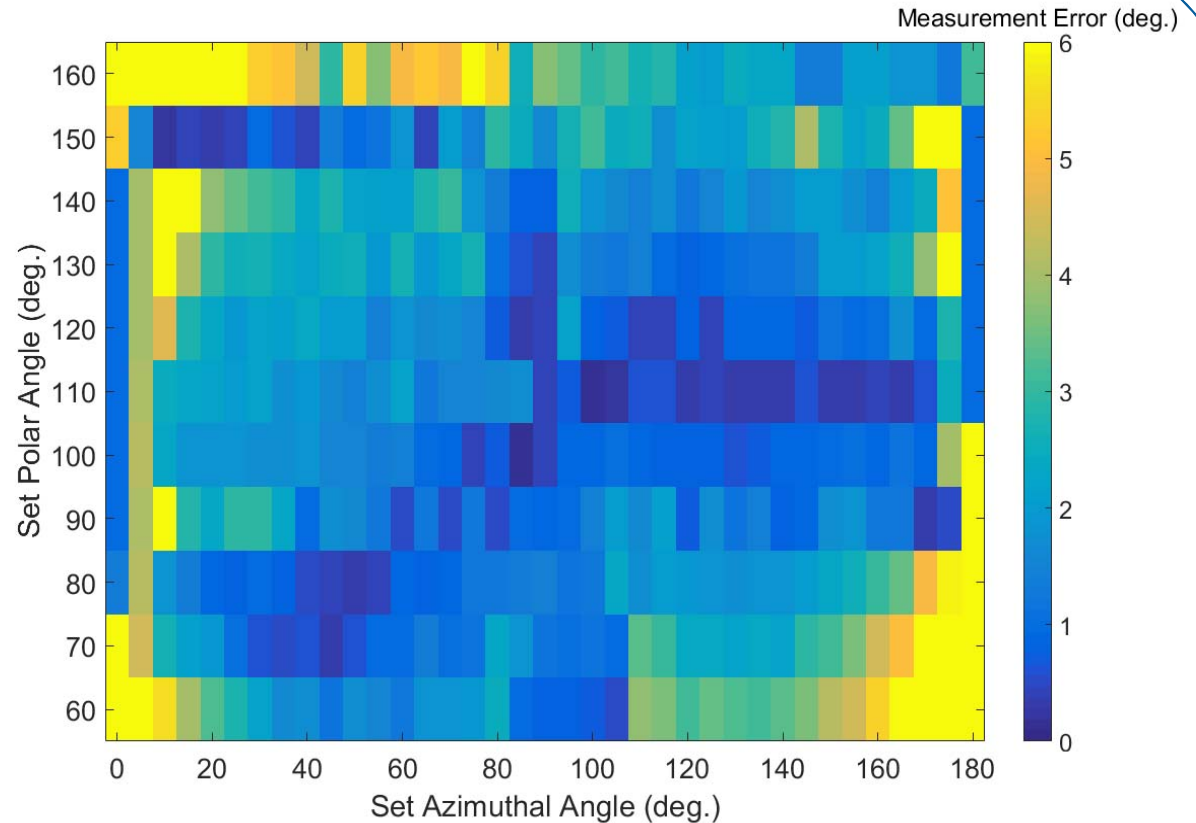
Measurement errors are well within 1° for most polar angles.

Advanced Signal Extraction

- Polar and Azimuthal Angle Measurement with two orthogonal sensors



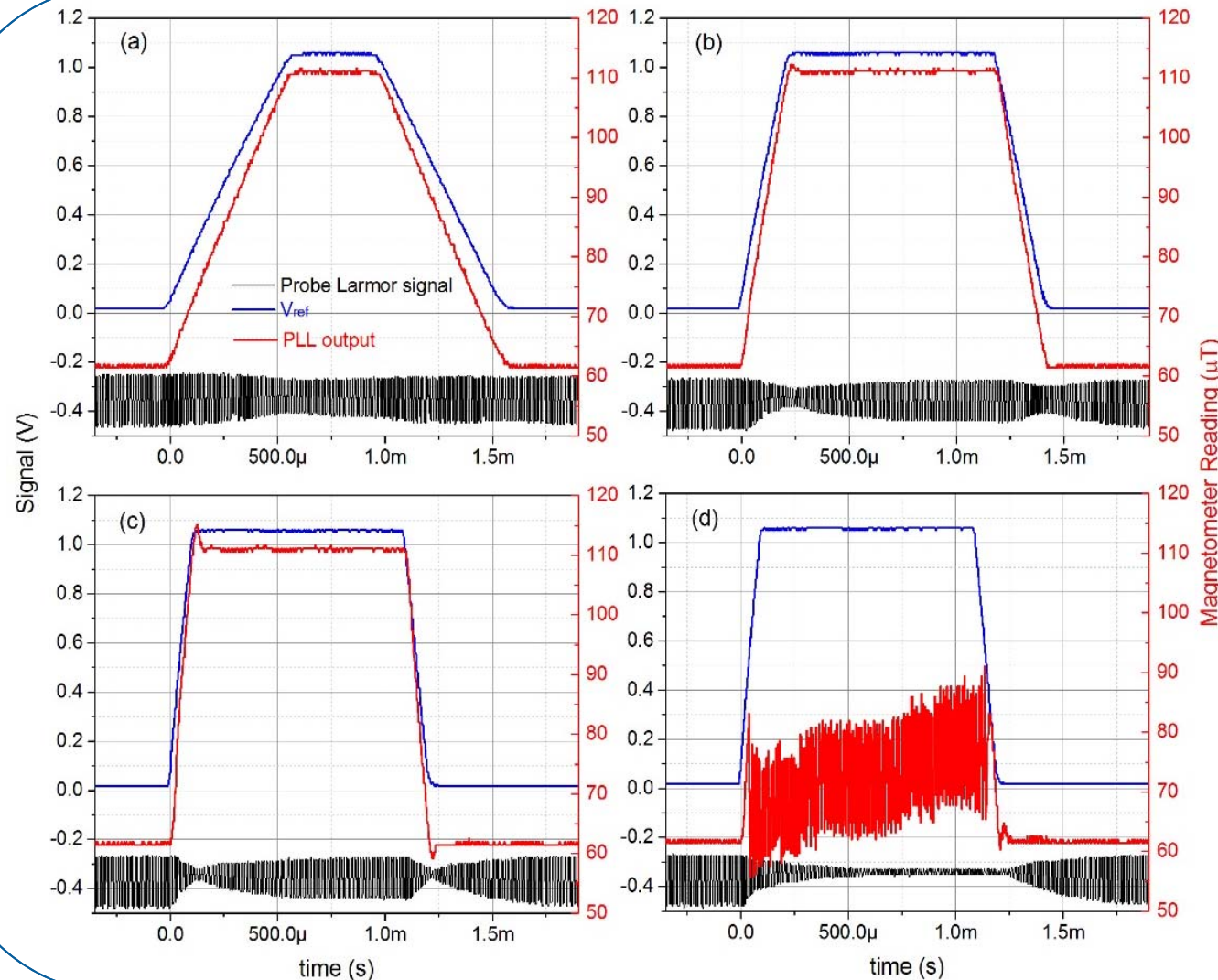
The coordinate is defined by sensor 1 and sensor 2. We rotate the coordinate to set the polar and azimuthal angle.



The Measurement Error is plotted as the color map.

Fast EM Pulse Recovery

- Dynamic Response of an Ultra-high Bandwidth Magnetometer



Ramping of a 50 μT magnetic field in (a) 500 μs , (b) 200 μs , (c) 100 μs and (d) 90 μs .

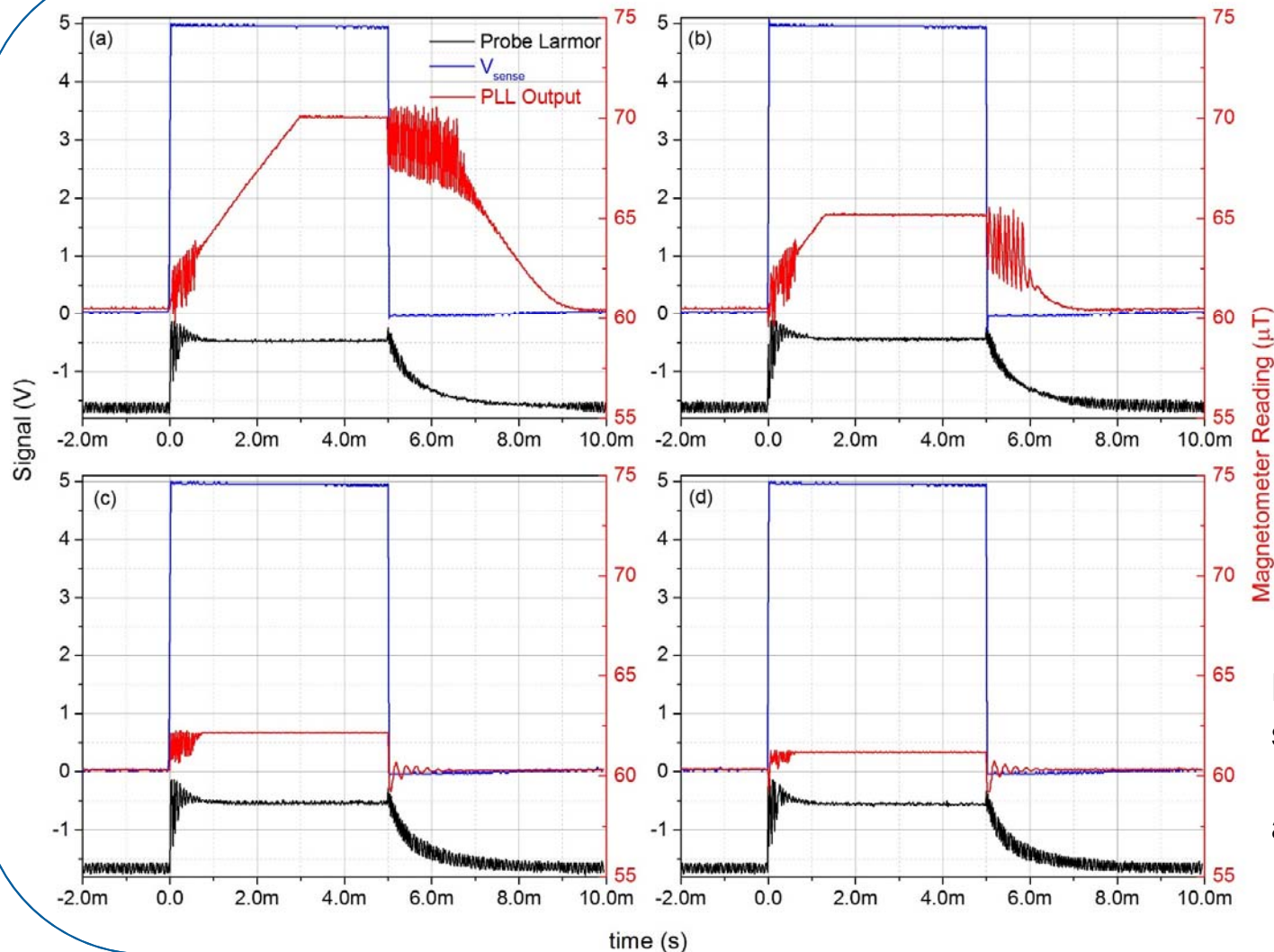
Black: Larmor Signal

Red: Magnetometer Output

Blue: Voltage drop on a resistor in series with the coil generating the field

Fast EM Pulse Recovery

- Most Promising Fast-recovery Method: Limiting PLL Range



When a fast change of field reading is detected, the PLL automatically sets a frequency limit on how much the pump modulation frequency is allowed to change from its original (before the fast change) frequency.

220 μT magnetic pulse with a 10 μs ramping time

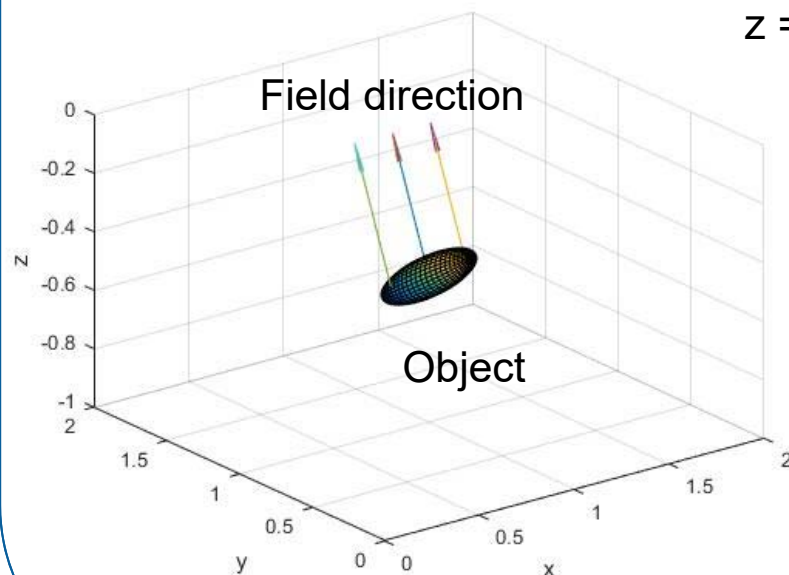
Frequency limitation set at (a) 35 kHz, (b) 17.5 kHz, (c) 7 kHz and (d) 3.5 kHz.

Magnetic Response to DC Excitation

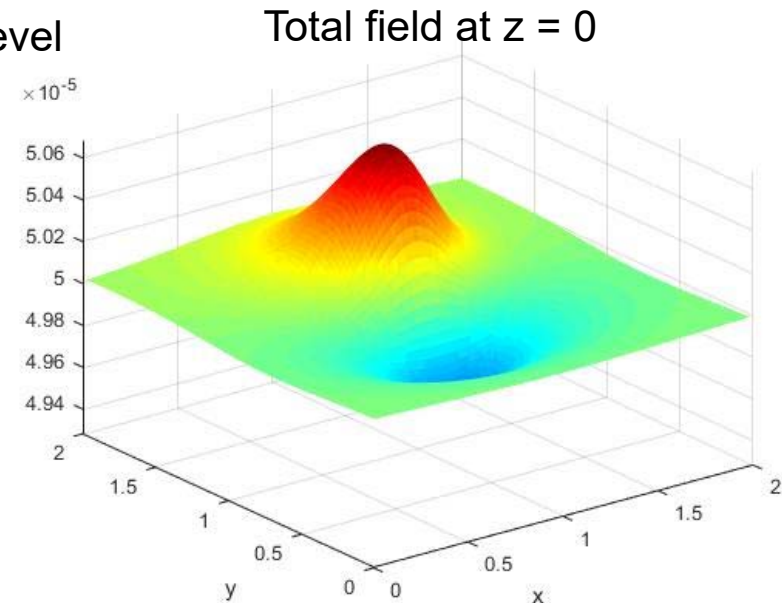
- Theoretical Model

Theoretical Model *

1. Cylindrically symmetric objects
2. Ferrous material without permanent magnetization
3. Dipole approximation for the induced magnetization: very good approximation when the magnetometer is more than two body lengths away from the object



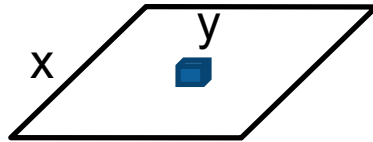
$z = 0$ ground level



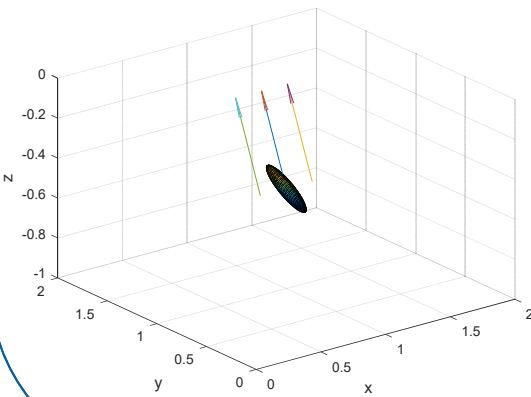
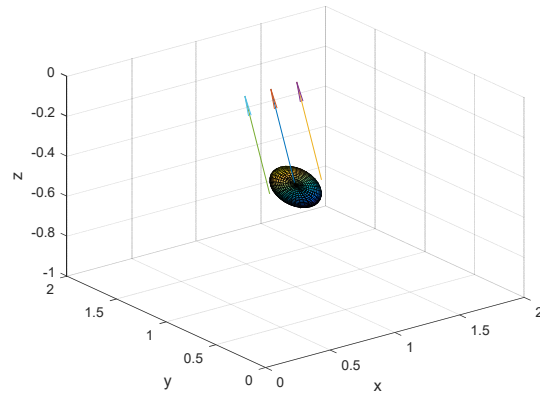
* Reference: S. D. Billings, L. R. Pasion, and D. W. Oldenburg, "Discrimination and Identification of UXO by Geophysical Inversion of Total-Field Magnetic Data", ERDC/GSL TR-02-16, U.S. Army Corp of Engineers, 2002.

Magnetic Response to DC Excitation

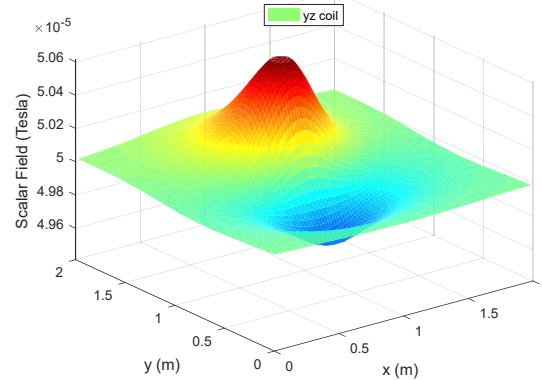
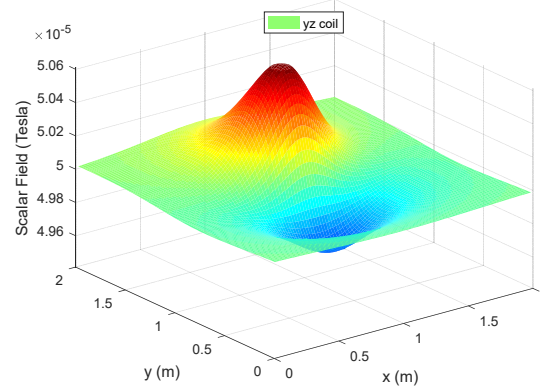
- UXO discrimination enhancement



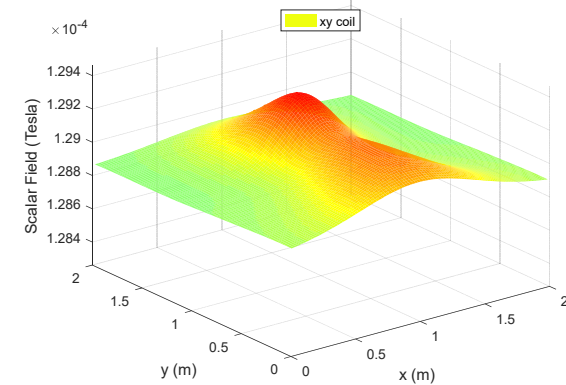
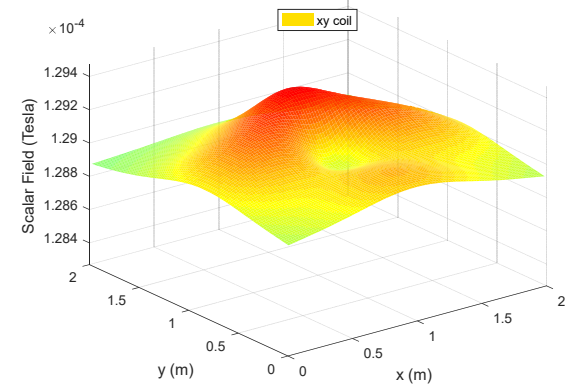
2m square coil, 200 μT field at the center of the coil



No additional field

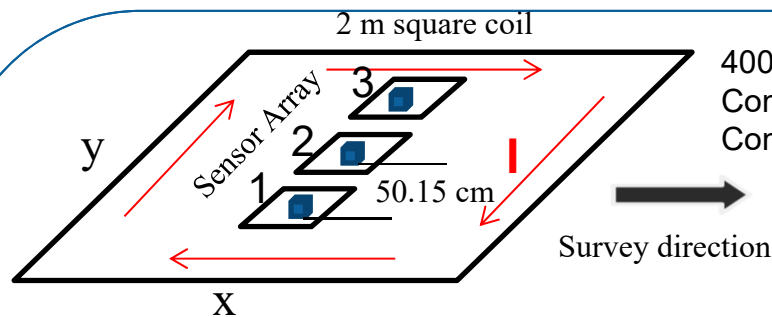


With coil on



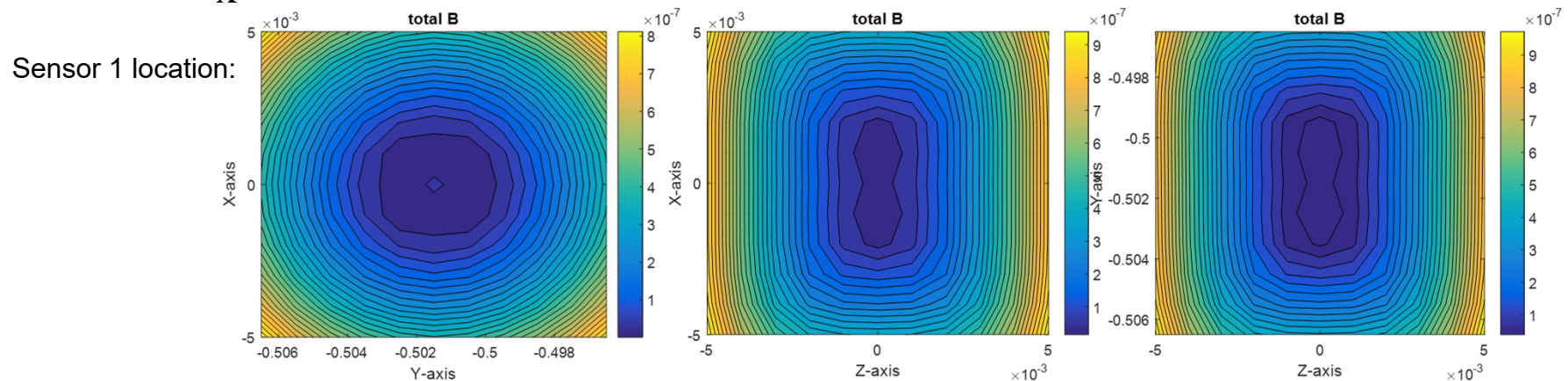
Magnetic Response to DC Excitation

- Practical design



400 A for the big coil and 50 A for the small coil.
 Compensation coil size: 20.4 cm and 24.6 cm
 Compensation coil center position: (0,-49.4 cm,0) and (0,0,0)

Magnetic field plot at sensor locations with coil energized



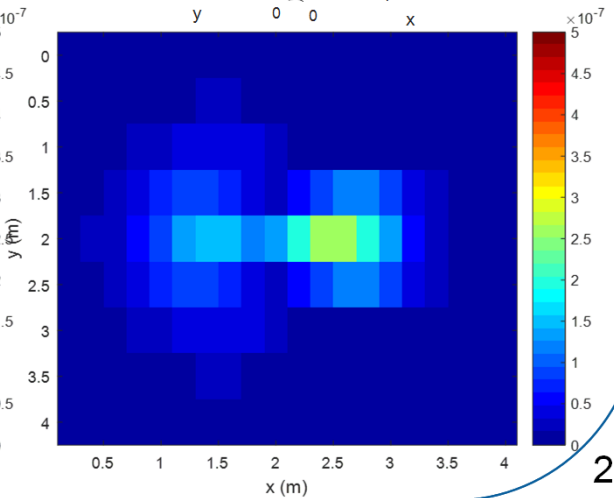
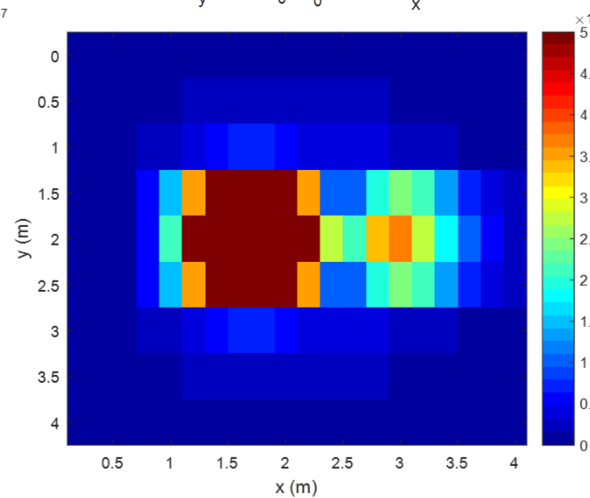
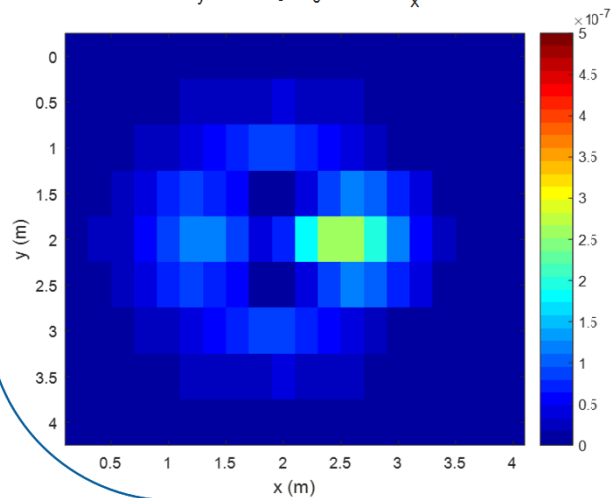
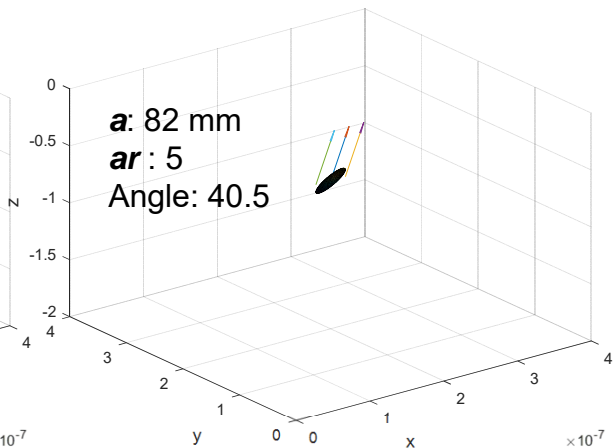
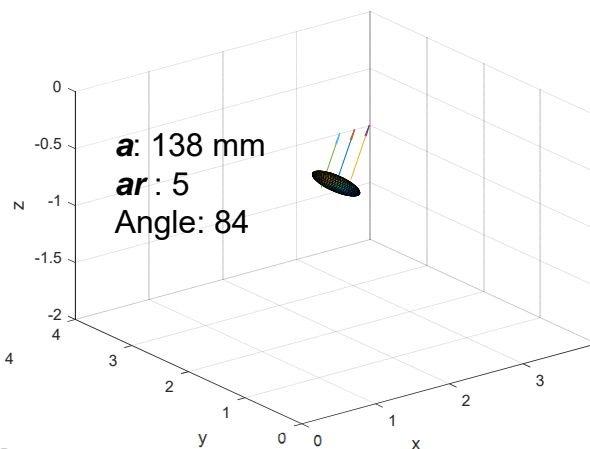
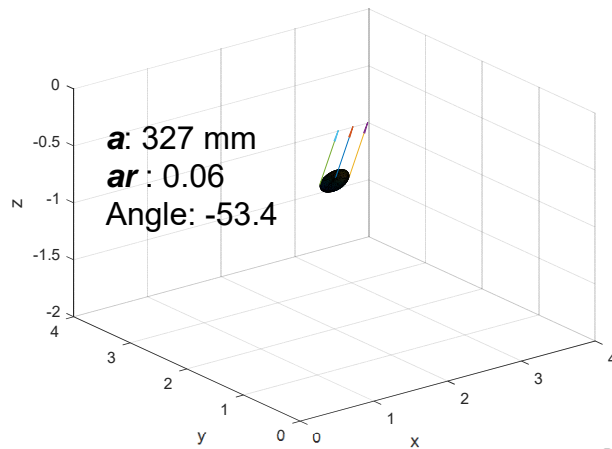
The heading error effect caused by the non-zero coil field at the sensor location can be further compensated once we know the angle information of the background field during the survey.

Magnetic Response to DC Excitation

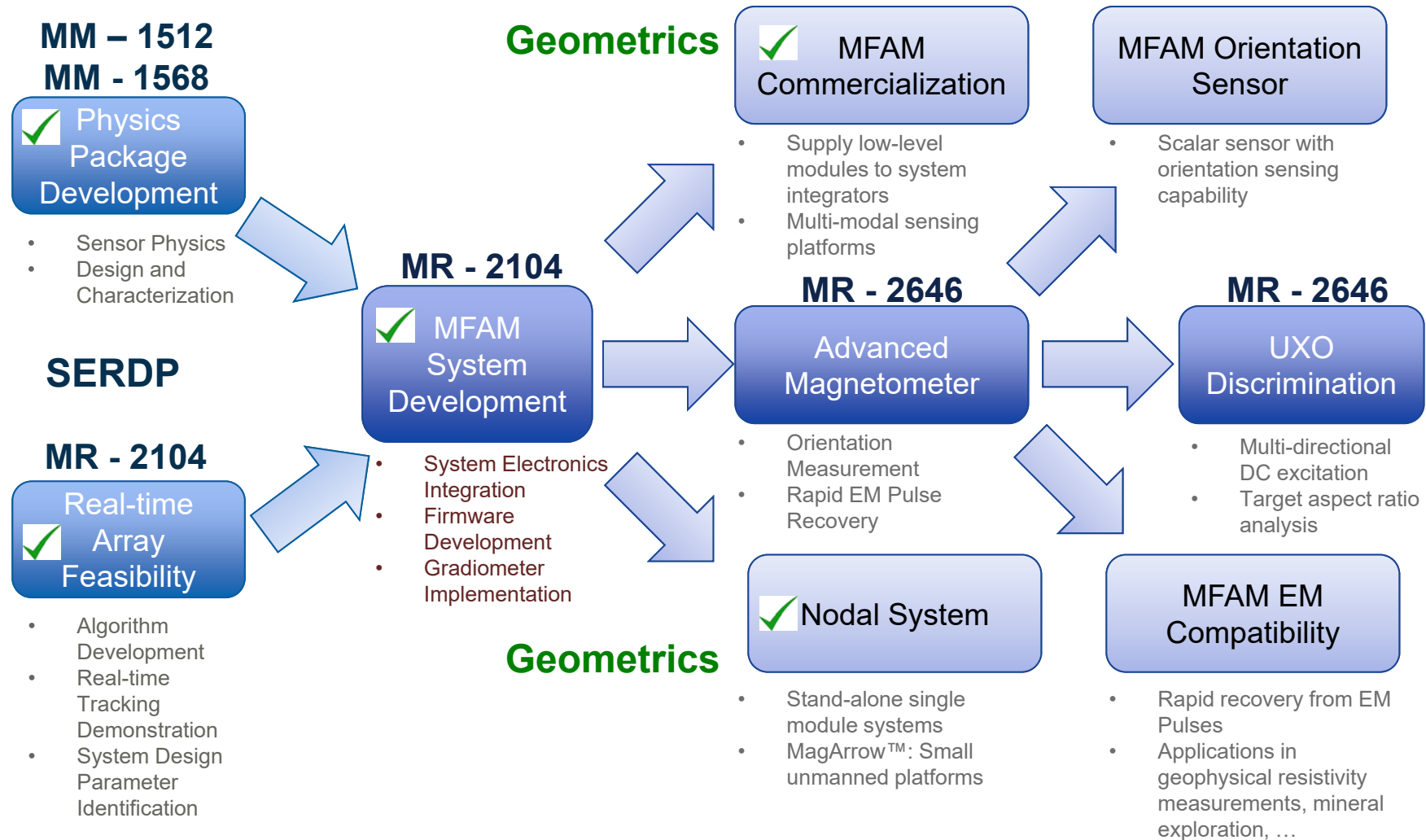
- Simulation results using 3 sensors and compensation coils

0.7 m deep

Objects are spheroids, characterized by the diameter a and aspect ratio ar (length = $a \cdot ar$). The angle between the symmetric axis and the background magnetic field ($50 \mu\text{T}$, in x-z plane, 30 degrees from vertical) varies.



Transition Plan



Issues

- We had to work through delays caused by resource constraints due to some Engineers leaving Geometrics and R&D effort being focused on commercialization of the MFAM technology, the development of which was partly supported by SERDP through projects MM – 1512, MM – 1568 and MR-2104.

Project Funding

	FY15*	FY17*	FY18*	FY15*	Total
Funds received or budgeted (\$K)	310	176	0 (306)		
% Expended	100	37	0		
Planned % Expended	100	75	0		
Funds Remaining (\$K)	0	110	0		

NOTE: If substantial funds remain from FY13 (or previous years), please contact your Program Manager in advance of the IPR.

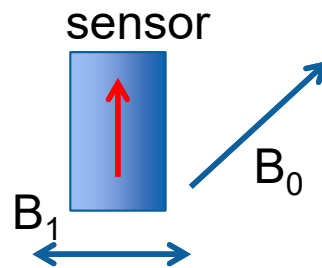
***NOTE: Include a column for all fiscal years in which funds have been or are planned to be received.**

BACKUP MATERIAL

These charts are required, but will only be briefed if questions arise.

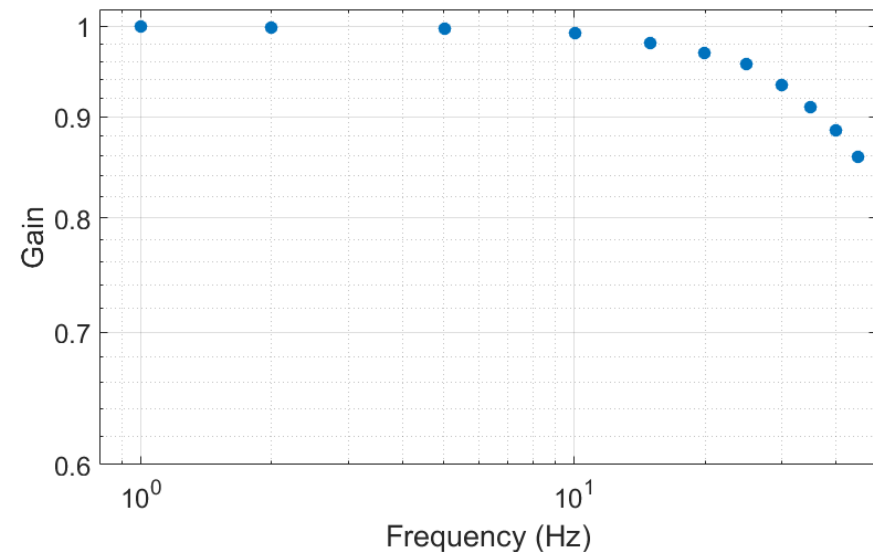
Advanced Signal Extraction

- Bandwidth of Polar angle measurement using Light Absorption Method



- Small oscillating field B_1 added to introduce a change in the polar angle.
- Frequency swept with fixed amplitude

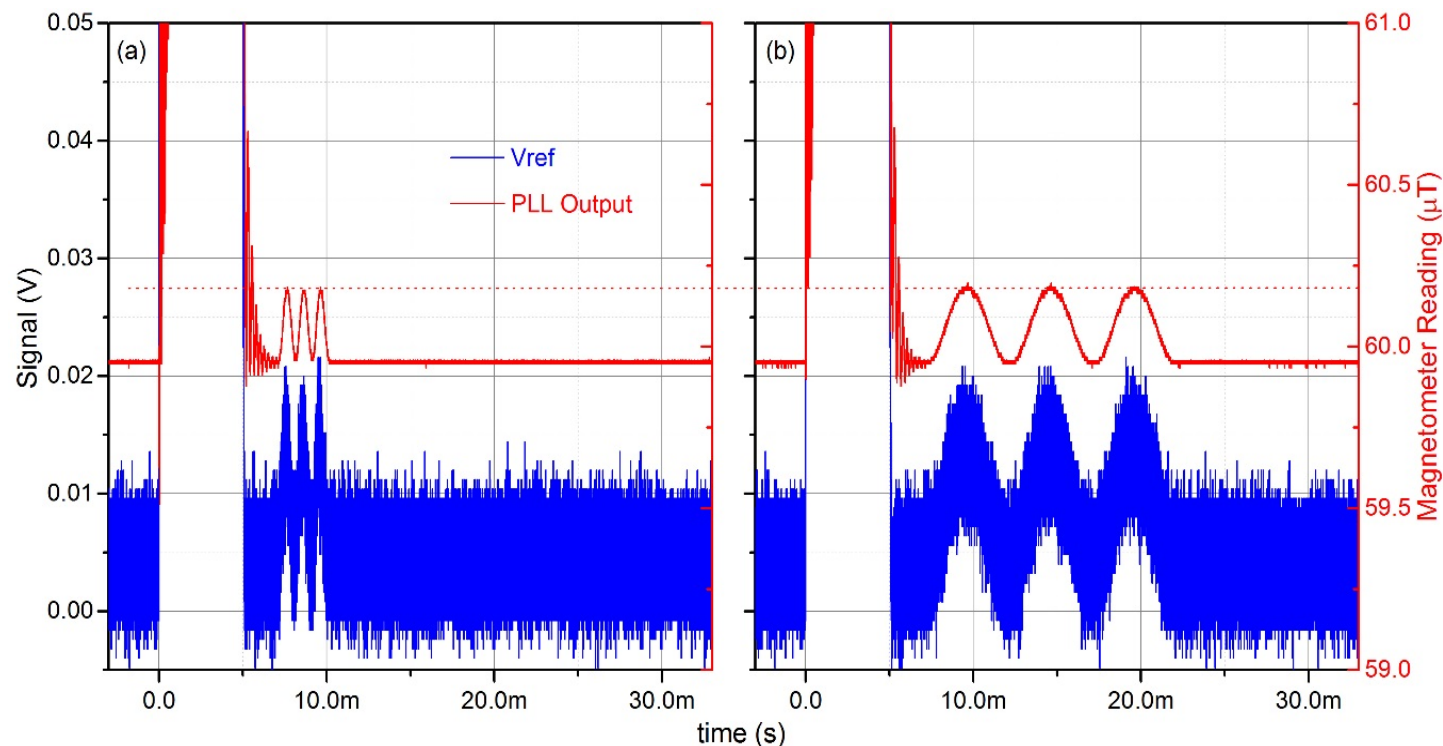
Bandwidth Characterization



The system bandwidth **well above 50 Hz**
 Currently limited by the 100 Hz sample rate anti-alias filter
 The measured polar angle oscillation amplitude is normalized.

Fast EM Pulse Recovery

- Field measurement after recovery



After the $220 \mu\text{T}$ field is turned off in less than $20 \mu\text{s}$ at $t = 5$ ms, a small oscillating field, ~ 200 nT, 3 cycles at 1 kHz (a) and 200 Hz (b), is applied (indicated by the blue curve). The magnetometer clearly responds to this field change. The expected field reading shows up in the magnetometer output.